Photoinduced Reaction of Digermane with Si(111)

Gregory J. Batinica and John E. Crowell*

Department of Chemistry and Biochemistry and Materials Science Graduate Program, University of California, San Diego, La Jolla, California 92093-0314

Received: June 15, 1999; In Final Form: September 7, 1999

The photoinduced reaction of digermane with the Si(111) surface using ultraviolet irradiation has been studied using temperature-programmed desorption (TPD) and Auger electron spectroscopy (AES). Hydrogen and germane desorption yields and relative Ge/Si AES signals are used to determine the reactivity of digermane. UV irradiation during or after dosing of the Si crystal surface at low temperatures (≤120 K) enhances the reactivity of digermane compared to similar doses without UV irradiation. Adsorption and photoexcitation of digermane at 110 K lead to significantly more reaction that at 120 K. We also find that UV irradiation after dosing the Si(111) surface with digermane enhances the reactivity more than simultaneous UV irradiation at 110 K, but the opposite is true at 120 K. Evidence is also found for precursor-mediated adsorption, and this is used to rationalize the dramatic changes with temperature. Photoexcitation of digermane at low temperatures leads initially to deposition of a-Ge:H.

1. Introduction

As demands on electronic device performance continue to grow, increased emphasis is placed on developing new and improved processing methods and materials. In particular, improving device performance by reducing device dimensions requires greater control on the structure, composition, uniformity, thickness, and physical properties of deposited thin films. The need for abrupt interfaces, doping level variations, and graded composition, for example, is placing even greater restrictions on processing conditions, and on the thermal budget. The search for new material compositions compatible with silicon technology is another active area of study aimed at improving device performance. Toward this end, an attractive and promising area of research and development has been high-speed electronic devices based upon silicon−germanium epilayers and heterostructures.[1]

$Si_{1-x}Ge_x$ alloys grown on Si substrates by CVD and molecular beam epitaxy (MBE) have been studied extensively using numerous techniques.[2−22] Some of the unique behavior observed for Si/Ge heterostructures is attributed to the 4% lattice mismatch between Si and Ge and the lower free energy of Ge surfaces relative to Si surfaces. $Si_{1-x}Ge_x$ alloys have also been grown by photoassisted CVD (PCVD) using Ge_2H_6/Si_2H_6 precursor gases and 193 nm laser pulses directed parallel to the surface at 548 K by Li et al.[23] The rate of $Si_{1-x}Ge_x$ growth was accelerated compared to nonphotoassisted conditions. Meyerson et al.[24] were the first to show that Ge had a catalytic cooperative effect on Si deposition. They found that the rates of both Ge and Si deposition were enhanced by increasing the Ge_2H_6/Si_2H_6 gas source ratio at a constant Si_2H_6 pressure. Ning and Crowell[25,26] explored the influence of Ge on the desorption of hydrogen from Si surfaces and the resulting enhancement in $Si_{1-x}Ge_x$ deposition and showed that the extent of the enhancement was correlated to the Ge concentration and to the resulting decrease in the H_2 desorption temperature, the rate-limiting step to Si deposition. In the photoassisted CVD study by Li et al.,[23] an even greater enhancement in Ge deposition resulted from photolytically activated Ge_2H_6 (which was believed to have an absorption cross-section *30 times greater* than Si_2H_6 at 193 nm) reacting more rapidly with the surface. Thus, increasing the Ge_2H_6 pressure, while also making the alloy more Ge rich, enhanced the growth rate of both Si and Ge.

Pure Ge layers have also been deposited onto Si substrates using MBE or CVD methods and various aspects of the deposition process or the resulting heterostructure have been studied.[27−41] The main CVD precursor gases studied have been Ge_2H_6, GeH_4, and $GeCl_4$. For the gaseous hydride precursors, CVD proceeds via (i) adsorption, (ii) decomposition, and (iii) desorption of hydrogen to free dangling bond sites for further deposition. $GeCl_4$ source gas deposition is similar, but chloride products are either thermally desorbed or etched away by hydrogen to free surface sites for further Ge deposition.[40,41] Film growth of Ge on Si is widely believed to proceed through the Stranski−Krastanov (S−K) growth mode with 3D islanding commencing after layer by layer growth of a few monolayers of Ge.

The thermal decomposition of Ge_2H_6 on Si(100) has been studied by TPD,[42−44] ultraviolet photoelectron spectroscopy (UPS),[43] X-ray photoelectron spectroscopy (XPS),[43] and multiple internal reflection infrared spectroscopy (MIRIRS).[45] The decomposition pathway is believed to begin with adsorption of a physisorbed molecular precursor followed by Ge−Ge bond scission by the Si dangling bonds, creating adsorbed GeH_3 species. The GeH_3 species subsequently decompose, forming GeH_x ($x = 1-3$) and SiH surface species. Decomposition of adsorbed GeH_3 can begin on Si at temperatures as low as 150 K. In comparison, the thermal interaction of disilane with the Si(111), Si(100), and Ge(111) surfaces has been studied by a variety of surface probes including MIRIRS,[46−51] electron energy loss spectroscopy (EELS),[52,53] UPS,[54,55] scanning tunneling microscopy (STM),[56] and molecular beam scattering.[57,58] Disilane follows a similar stepwise decomposition on these surfaces as Ge_2H_6 does on the Si(100) surface, that is, molecular

* To whom correspondence should be addressed: Phone: (858) 534-5441. FAX: (858) 534-7244. E-mail: jcrowell@ucsd.edu.

10.1021/jp991978p CCC: $18.00
Published on Web 11/18/1999

physisorption followed by Si−Si bond scission and formation of $SiH_{3(ads)}$ followed by stepwise decomposition of $SiH_{3(ads)}$. When a silicon surface is exposed to various Si and Ge hydride gases, the surface will become passivated because the surface dangling bonds will ultimately be fully consumed, provided the substrate temperature is below that of hydrogen desorption. This passivation has been seen from disilane uptake curves with Si(100),[59,60] Si(111),[61] and with Ge_2H_6 on Si(100),[43] where the uptake curves are characterized by a rise as a function of exposure at small dosages but then level off as the dosage increases. The use of GeH_4 and Ge_2H_6 as precursor gases for epitaxial CVD growth of Ge on Si require temperatures greater than the hydrogen desorption temperature, since H_2 desorption is required to liberate the surface sites needed for further reaction of the deposition precursors[51] (at extremely high temperatures adsorption is the rate-limiting step rather than H_2 desorption). Although it is well-known that Ge reduces the desorption temperature of hydrogen from Si,[25,26,50,62−65] high temperatures are still required for efficient epitaxial growth. In the fabrication of electronic devices, high temperatures can cause diffusion and undesirable solid-state reactions to occur. *In devising ways to precisely control epitaxial growth layer by layer while ensuring abrupt interfaces, lower temperature processing methods need to be found. Our photoinduced deposition studies focus on exploring this issue at a fundamental level.*

In this paper we examine the photoinduced reaction of digermane with Si(111) at low temperatures. We compare the deposition induced by UV excitation to that which occurs thermally. We also compare the effect of temperature and UV exposure conditions on the deposition efficiency. The relative quantity of digermane reacting with a silicon surface can be determined by hydrogen and germane TPD desorption yields and by relative Ge/Si Auger electron spectroscopy (AES) signals. We explore the reactivity of Ge_2H_6 on Si(111) with UV irradiation directed perpendicular to the crystal face during or after Ge_2H_6 dosing and give a plausible mechanistic explanation for our observations. The purpose of this study is to explore ways of depositing Ge/Si and $Si_{1-x}Ge_x$ semiconductor films at a reduced thermal budget.

2. Experimental Methods

Experiments were performed in an ultrahigh vacuum chamber with a base pressure of approximately 2×10^{-10} Torr. Details of the chamber design have been described previously.[66] The Si(111) samples were cut from n-type Si(111) wafers, of 5−20 mΩ cm resistivity. The temperature was measured by a chromel−alumel thermocouple that was attached to the back of the crystal using a ceramic adhesive (Ultra-Temp 516, Aremco Products, Inc.). The ceramic adhesive was cured at a high temperature (ca. 1350 K) under an applied pressure provided by tantalum tabs. The ceramic adhesive served to electrically isolate the thermocouple from the crystal and to presumably prevent the diffusion of Ni from the thermocouple into the Si. Routine cleaning of the silicon sample before each experiment was performed by Ar^+ ion bombardment (1 keV, 2.5 μA) at 575 K followed by annealing at 1140 K for 3 min. Surface cleanliness was checked by AES using a CMA, and impurities (carbon and oxygen) after preparation were well within the noise level of the spectrometer.

TPD studies were performed by resistively heating the Si crystal at a rate of 3 K/s (using a Eurotherm temperature controller with a high current/high voltage power supply) while positioned within a few millimeters of the orifice of a shielded quadrupole mass spectrometer (QMS). The temperature and the mass/charge ratios were monitored during the desorption using a computer interfaced to the QMS. Amu 2 was monitored for the H_2 desorption yields and amu 76 for the GeH_4 desorption yields. Amu 76 is the most abundant cracking fragment (GeH_2^+) of germane for the most abundant isotope (^{74}Ge) of germanium.

A white-hot (1757 K) tungsten filament placed approximately 5 cm from the crystal surface was used to produce atomic hydrogen during exposure of H_2 (Liquid Air Corp., research grade, 99.9999%). Commercial digermane (Voltaix, UHP grade purity, 99.999% excluding a 0.5% concentration of GeH_4 and Ge_3H_8) was used as purchased without purification. All exposures are given in langmuirs (1 langmuir = 10^{-6} Torr s) of the molecular source gas, and are uncorrected for ion gauge sensitivity. H_2 desorption yields were normalized to that of a complete H-monolayer (i.e., $\Theta_H = 1.0$) prepared by exposing the Si(111) surface to 300 langmuirs of H/H_2 at 640 K: this exposure procedure resulted in a saturated β_1 (surface monohydride) desorption state with no β_2 (dihydride) desorption. The germanium concentration of the surface was measured by AES using the Si LMM 92 eV transition and the Ge LMM 1147 eV transition. Surface composition was determined by ratioing each component's Auger intensity to the sum of all elements' Auger intensities, using Auger sensitivity factors taken from a standard source.[67] Actual surface concentrations of Ge may be higher than the reported values due to contributions from the bulk or due to possible 3D growth of Ge.

A commercially available D_2 lamp with a MgF_2 window (Hamamatsu Photonics, L879, 30 W, spectral range 115−300 nm, peak emission at 161 nm) was used as the UV light source. The lamp was positioned inside the vacuum chamber fully encased in a copper housing. To minimize outgassing due to the temperature rise of the lamp during illumination, the Cu housing was cooled by ice from the outside via a solid copper feedthrough. During illumination, the Si crystal was placed approximately 2 cm from the lamp's MgF_2 window, in a vertical position. The digermane dosing pressure was 5×10^{-8} Torr.

3. Results

In this study, we compare the thermal and photoinduced reaction of digermane on Si(111) at 110 and 120 K. These temperatures were chosen due to the relatively low desorption temperature for molecular digermane and due to difficulties in consistently maintaining temperatures <110 K. Although we did not directly measure the digermane molecular desorption temperature, we can make a good estimate of it. In our laboratory we have observed that molecular Ge_2H_6 desorbs from Si(100) at 145 K,[44] and molecular Si_2H_6 desorbs from Si(100) at 160 K[59] and from Si(111) at 147 K.[61] Hence, because disilane desorbs 13 K lower from Si(111) than Si(100), we estimate that Ge_2H_6 desorbs from Si(111) somewhat lower than from Si(100), namely, between 130 and 145 K; this is consistent with the pressure increase observed in the chamber upon initiating TPD measurements for digermane-dosed Si(111) surfaces.

3.1. Thermal Reactivity of Ge_2H_6 on Si(111). The thermal reaction of digermane on Si(111) was studied at 110 and 120 K. After adsorption, the surface was heated linearly at 3 K/s and the hydrogen and germane desorption signals were recorded. Only hydrogen was observed to desorb; no germane desorbed from the Si(111) surface under thermal reaction conditions for exposures ≤40 langmuirs. Representative hydrogen desorption spectra following digermane adsorption at 110 K and subsequent decomposition are given in Figure 1A. The H_2 TPD spectra display two prominent features, the β_1 and α desorption states. Initially, at low digermane exposures, only the β_1 feature at

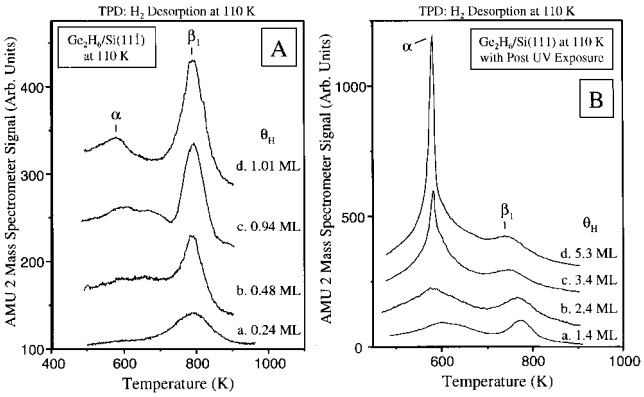

Figure 1. H_2 TPD spectra from digermane adsorption on Si(111) at 110 K: (a)−(d) digermane dosages of 2, 5, 10, and 25 langmuirs, respectively. The thermal reaction of digermane (A) is compared with the photoreaction (i.e., adsorption and post-UV exposure) of digermane (B) at 110 K. The surface coverage (Θ_H) is determined by integrating the desorption area and comparing it to a saturated monohydride monolayer.

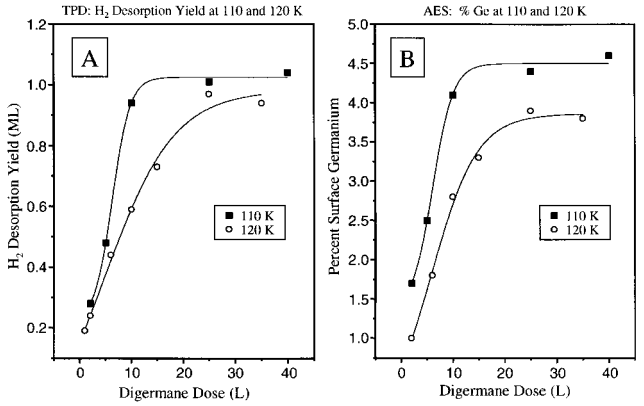

Figure 2. H_2 TPD desorption yield (A) and % Ge AES signal (B) as a function of digermane exposure of Si(111) under thermal reaction conditions at 110 K (■) vs 120 K (○). The hydrogen desorption area in (A) is normalized to the area of an H-monohydride monolayer on Si(111).

~780 K is observed, but at moderate exposures (5−10 langmuirs), an additional broad, weak feature begins to appear near ~600 K; this is termed the α desorption state. The β_1 state is due to the decomposition of two silicon monohydride species (SiH), producing β_1-H_2 and two dangling bonds. The α state is due to desorption of hydrogen from Ge sites.[25,26,44,63,64,68] At higher Ge_2H_6 exposures, the β_1 state nears saturation, and a small yet distinct α state is evident, peaked at 580 K. Integration of the TPD spectra provides a measure of the extent of reaction. The amount of hydrogen that desorbs is then normalized with respect to the saturation coverage of hydrogen present in a monohydride monolayer (equivalent to the number of dangling bonds present on Si(111)), to give the hydrogen coverage, Θ_H, in monolayers. The reaction probability can be estimated from the normalized hydrogen desorption yield (Θ_H), assuming that the Si(111) surface density[69] is 7.83×10^{14} atoms/cm^2, and correcting the digermane exposure using an ion gauge sensitivity of digermane relative to nitrogen of 2.4.[70] We find that less than 20% of the physisorbed digermane at 110 K dissociates upon heating.

In Figure 2 we compare the hydrogen desorption yield and the percent of surface germanium, as measured by AES, for digermane adsorption at 110 vs 120 K. Upon adsorption at 120 K, we observe that the hydrogen desorption yield and the % Ge AES curve rise more slowly and level off at a lower hydrogen yield and less deposited Ge, respectively, than at 110 K. This indicates that the *thermal reactivity* of digermane is *greater* on Si(111) at a substrate temperature of 110 K than at 120 K. We find that at 120 K, about 15% of the physisorbed digermane leads to hydrogen production. The reaction probability differences at 110 vs 120 K are also reflected in the amount of germanium that gets deposited, as shown in the AES data of Figure 2B.

3.2. Photoreaction of Ge_2H_6 on Si(111). The photoinduced reaction of digermane on Si(111) was studied at 110 and 120 K. For both temperatures, three series of experiments were performed: (i) the crystal face was irradiated while dosing with digermane at 5×10^{-8} Torr (termed "simultaneous UV exposure"), (ii) the crystal face was irradiated after digermane exposure (termed "post-UV exposure", with the duration of the irradiation being the same as that for the comparable simultaneous UV exposure for a given digermane dose), and (iii) the crystal surface was not irradiated either during or after digermane exposure (termed "no UV" exposure). Hydrogen and germane TPD yields and the percent of surface Ge, determined by AES, were plotted as a function of digermane dosage. The desorption yields of hydrogen and germane, along with the percent of surface Ge, correlate with the amount of Ge_2H_6 that reacts with the Si surface. Furthermore, the change in relative germanium hydride (α) and silicon hydride (β_1 and β_2) desorption yields as a function of the total hydrogen yield also gives a good indication of the extent of germanium deposition.

The TPD spectra shown in Figure 1A depicting digermane thermal decomposition following adsorption at 110 K illustrate that H_2 desorption occurs primarily from the silicon hydrides. This is sharply contrasted by what occurs upon photoexcitation following similar digermane exposures. Figure 1B shows representative TPD spectra under high reactivity conditions, namely TPD spectra upon exposing Si(111) to digermane at 110 K and then subsequently exposing the surface to UV irradiation. Two TPD features are again observed: the β_1 and α desorption states. However, in this case, photoexcitation leads to significantly more hydrogen desorption in general, and in particular, a substantial increase in the relative α-H_2 desorption from Ge atoms with increasing exposure compared to β_1-H_2 desorption from Si sites. In addition, the β_1 and α TPD features both shift to lower temperatures with increasing exposure; this behavior is typical of hydrogen desorption from Ge/Si surfaces.[25,26] The width of the α-H_2 desorption state also narrows considerably with increasing UV and digermane exposure (fwhm = 15 K for the 25 langmuir exposure). This behavior is distinct from that occurring for α-H_2 desorption from Ge/Si(100)[25,26] or Ge/Si(111)[60] surfaces, where the α-H_2 state is much broader. However, in this case (Figure 1B), a much greater amount of hydrogen is desorbing from the surface. Similarly shaped TPD spectra were seen for the photoreaction of digermane on the Si(100)-2×1:D surface.[44] Under photoreaction conditions, hydrogen desorption (Figure 1B) from Si(111) is preceded by a symmetric and intense GeH_4 desorption state peaked at 550 K, similar to that observed on Si(100).[44]

3.3. Adsorption of Ge_2H_6 at 110 K. *Ultraviolet irradiation* greatly enhances the reactivity of digermane with Si(111) at 110 K compared to the *thermal reaction* of digermane with Si(111) at this temperature. The H_2 and GeH_4 desorption yields are plotted as a function of digermane exposure in Figure 3A,B, respectively, for the three dosing conditions described above. The corresponding AES data are plotted in Figure 3C. Examination of the uptake curves in Figure 3 shows a strong UV photoreaction enhancement throughout the range of dosages

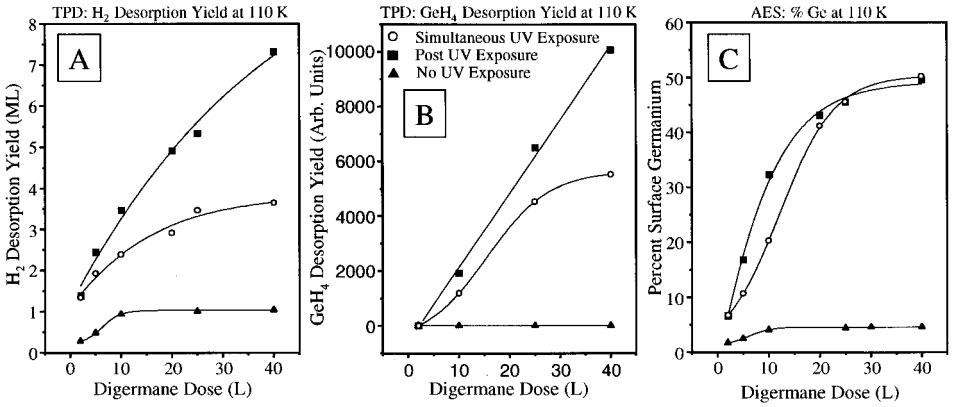

Figure 3. H_2 (A) and GeH_4 (B) TPD desorption yields and % Ge AES signal (C) as a function of digermane dose of Si(111) at 110 K under various UV-excitation conditions: simultaneous UV (○), post-UV (■), and no UV (▲) exposure. The H_2 TPD area in (A) is normalized to the area of an H-monohydride monolayer on Si(111).

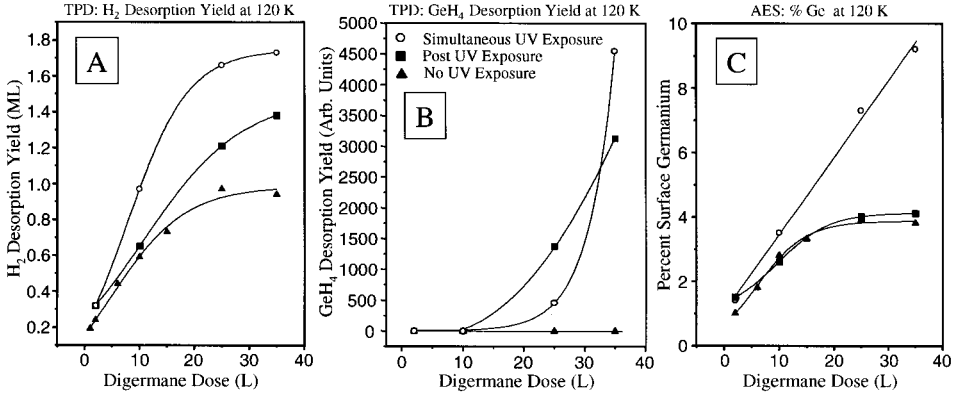

Figure 4. H_2 (A) and GeH_4 (B) TPD desorption yields and % Ge AES signal (C) as a function of digermane dose of Si(111) at 120 K under various UV-excitation conditions: simultaneous UV (○), post-UV (■), and no UV (▲) exposure. The H_2 TPD area in (A) is normalized to the area of an H-monohydride monolayer on Si(111).

examined. Post UV irradiation enhances the reactivity of digermane more than simultaneous UV irradiation, and both are substantially greater than reaction without UV irradiation. The H_2 desorption yields (Figure 3A) are about one monolayer for the thermal (non-UV assisted) reaction of digermane with Si(111), while for simultaneous UV exposure, the H_2 desorption yield reaches more than 3 times that for a 40 langmuir digermane exposure. For post-UV exposure at 110 K, the desorption yield reaches over seven monolayers of desorbed hydrogen and does not level off for the range of dosages presented (Figure 3A). Germane desorption (Figure 3B) shows a trend similar to that observed for H_2 desorption: post-UV excitation results in substantial GeH_4 production, whereas simultaneous UV exposure at 110 K results in significant but less GeH_4 production. No germane desorption occurs for the thermal reaction of digermane with Si(111) at the digermane exposures utilized here ($\leq$40 langmuirs). The observation of substantial GeH_4 desorption, along with the desorption of more that 7 monolayers of H_2 following photoexcitation of a moderate Ge_2H_6 dose ($\sim$10 langmuirs, correcting for ion gauge sensitivity) at 110 K, suggests growth of an a-Ge:H overlayer at these temperatures, as discussed below (section 4.4).

The curves shown in Figure 3C, illustrating the % Ge deposited as measured by AES, also indicate the large enhancement UV irradiation has on the reaction of digermane with Si(111) and display a trend similar to that seen in Figure 3A,B. However, at high Ge coverages, both simultaneous UV and post-UV assisted growth display similar Ge deposition yields. This result is distinct from that observed by TPD (cf. Figure 3C vs Figure 3A). This is probably due to 3D islanding of Ge on the Si surface or due to Ge−Si intermixing,[65] both of which affect (lower) the Ge AES detection sensitivity, but not due to evaporation of Ge, since desorption of germanium from Si does not commence until about 1100 K.[71] The AES-derived Ge coverages plotted in Figure 3C were obtained after the digermane-exposed Si(111) surface was heated to 938 K to perform the TPD analysis.

3.4. Adsorption of Ge_2H_6 at 120 K. For digermane and UV exposures *at 120 K*, we also find that UV irradiation during or after Ge_2H_6 exposure increases the reactivity of digermane with Si(111) compared to similar digermane dosages without UV irradiation (Figure 4). However, in comparison to exposure at 110 K (Figure 3), the magnitude of the photoenhancement is significantly reduced. In particular, note that the H_2 and GeH_4 desorption yields are reduced by factors of ca. 4 and 2, respectively, upon increasing the adsorption temperature from 110 to 120 K, while the % Ge decreases by a factor of 5. Furthermore, we find that at 120 K, simultaneous UV irradiation enhances the reactivity of Ge_2H_6 with Si(111) more than post-UV irradiation, opposite to that found at 110 K. From the hydrogen desorption yields (Figure 4A) and the Ge surface coverage determinations (Figure 4C), we see in comparing the simultaneous UV and no UV irradiation curves that there is a small but noticeable UV effect at low digermane dosages, while at higher dosages the H_2 yield and Ge surface coverage for the simultaneous UV reaction are approximately double those of the thermal reaction. For post-UV exposure, the H_2 desorption yield (Figure 4A) is about halfway between that of simultaneous UV exposure and no UV exposure. However, the increase in % Ge deposited, as measured by AES, is only modestly greater

for post-UV exposure than that for the non-UV assisted reaction (Figure 4C). The germane desorption yields are plotted in Figure 4B; note that no germane desorption was observed at these rather low digermane exposures without the addition of UV irradiation. The post-UV and simultaneous UV assisted reactions show desorption of germane at moderate digermane dosages (>25 langmuirs), indicating that UV irradiation increases the reactivity of digermane with Si(111), but little can be inferred from this plot about the relative enhancement of reactivity by post-UV irradiation versus simultaneous UV irradiation.

4. Discussion

4.1. Comparison with Previous Studies. In previous studies by our group and others involving disilane adsorption on Si(100)[59] and Si(111)[46,53,61] and involving digermane adsorption on Si(100)-2×1:D,[44] the following three conclusions were made. (1) Adsorption occurs via a physisorbed precursor state.[46,53] In these thermal studies at low temperatures it was found that disilane molecularly adsorbs on the Si(111) surface at low temperatures and then dissociatively chemisorbs upon heating, with a small and negative apparent activation energy. Because of this molecular precursor state, one sees more disilane chemisorption when disilane is initially adsorbed at lower temperatures than at higher temperatures. (2) The photoinduced deposition reaction is mainly driven by SiH_2[59,61] and GeH_2[44] diradicals; these species are capable of inserting into existing Si−H and Ge−H surface bonds. In contrast, the thermal reactions of disilane and digermane are limited on silicon surfaces by the availability of surface dangling bonds. Once these gases chemisorb and consume all the surface dangling bonds, further (thermal) reaction is not possible unless hydrogen is desorbed and dangling bond sites are liberated; this is not possible at the low adsorption temperatures utilized here. Thus, deposition chemistry driven by photogenerated diradicals can increase digermane and disilane reactivity well beyond the thermal limit at low temperatures. (3) Under photoassisted conditions, condensed phase photolysis is occurring rather than gas-phase photolysis. In studies of the photoinduced reaction of disilane on Si(100)[59] and Si(111)[61] and of digermane on Si(100)-2×1:D,[44] it was found that physical adsorption of the molecular precursor was necessary for photochemical enhancement to occur. Evidence for condensed phase photolysis included (i) lack of photoenhancement if the substrate temperature exceeded the molecular desorption temperature, (ii) lack of photoenhancement if only the gas phase (and not the condensed phase) was irradiated, and (iii) similar photoenhancement upon adsorption and irradiation of either Si(100) or Si(100)-2×1:D.

We now show that the behavior described above is also consistent with our observations for the thermal and the photoinduced reaction of digermane with the Si(111) surface. The primary observations for this adsorption system can be summarized as follows:

(i) The thermal reaction of digermane on Si(111), induced upon heating the surface following exposure to digermane at temperatures at or above 110 K, results in H_2 desorption and Ge deposition. The hydrogen desorbs in two states (β_1 and α). The relative quantity of each of these desorption states is dependent on the initial digermane exposure. These states shift to lower desorption temperature with increasing Ge coverage, similar to that observed for H_2 desorption from Ge/Si(100) surfaces.[25,26,50,62−65]

(ii) Germane desorption is not observed for low digermane exposure under thermal conditions and is only observed under UV-assisted conditions. It is expected that germane desorption requires germyl (GeH_3) species to be present on the surface just prior to germane desorption, analogous to silane desorption.[44] Hence, we conclude that the lack of germane desorption indicates that germyl species are not present on Si(111) upon digermane exposure (at ≤40 langmuirs) at low temperature and upon heating to ca. 500 K. The fact that the H_2 yield saturates at 1 monolayer for digermane adsorption at 110 K illustrates that only enough digermane reacts thermally to generate a H/Si ratio of 1:1. Consequently, much of the digermane adsorbed at 110 K must desorb molecularly rather than dissociatively chemisorb. However, the data show that under UV-assisted conditions, much greater reaction occurs, resulting in all dangling bonds being saturated with H, GeH_x, or Ge_xH_y species and resulting in a-Ge:H deposition with increasing exposure.

(iii) The extent of thermal reaction of digermane, as measured by TPD, decreases as the temperature is raised from 110 to 120 K. The temperature-dependent uptake curves (Figure 2A) resemble those observed by Imbihl et al.[53] for disilane adsorption on Si(111) and suggests a negative apparent activation energy for the Ge_2H_6/Si(111) system as well. This, in turn, provides evidence of the presence of a physisorbed precursor state.

(iv) Photoinduced reaction of digermane, using either simultaneous UV irradiation during digermane exposure or UV exposure following digermane adsorption, results in a greater extent of reaction than that which occurs thermally. Furthermore, the extent of digermane photoreaction on Si(111) is significantly greater at 110 K than at 120 K. In addition, the timing of the UV irradiation relative to dosing affects the enhancement. In particular, post-UV irradiation of digermane adsorbed on Si(111) is more effective at inducing reaction and Ge deposition at 110 K than is simultaneous UV excitation, whereas the opposite is true at 120 K.

4.2. Thermal Reaction of Digermane on Si(111): Evidence for a Molecular Precursor State. Adsorption of digermane onto Si(111) at temperatures below the molecular digermane desorption temperature results in ≤1 monolayer of adsorbed hydrogen upon heating and thermal decomposition. We estimate that, at 110 K, less than 20% of the adsorbed digermane leads to decomposition; this value falls to 15% upon adsorption at 120 K. The uptake curves in Figure 2A resemble those observed previously for disilane adsorption on Si(111).[46,53,72] These results are pertinent, since the surface chemistry of disilane and digermane upon adsorption and reaction with the (111) faces of Si and Ge are quite similar.[46,48,73] In all of these studies, including the work presented here, the sticking coefficient decreases with increasing temperature, suggesting an adsorption process with a negative activation energy. Estimates of this negative apparent activation energy using either TPD or MIRIRS have been made: for disilane on Si(111), values of −1.7,[53] −1.9,[46] and −2.6[72] kcal/mol have been reported; for disilane adsorption on Ge(111), we estimate a value of −2.0 kcal/mol from MIRIRS studies.[74] An Arrhenius analysis of the uptake measurements derived from the TPD data given in Figure 2A gives an estimate of −0.8 kcal/mol for digermane adsorption on Si(111); this value is of similar magnitude to that observed for disilane on this surface.

4.3. Role of the Physisorbed Molecular Precursor State. The measurement of a negative apparent activation energy suggests that a weakly bound (physisorbed) molecular precursor state exists. The digermane molecules can dissociate from this physisorbed precursor state upon finding the correct binding site. The lower the temperature, the greater the residence time of the molecule in the physisorbed state, and the more likely it

is that the molecule can diffuse to find an appropriate bonding configuration that will lead to dissociation. This is reflected in the increased thermal reactivity seen at 110 vs 120 K. With UV excitation, there is also a tremendous increase in digermane reactivity at 110 K relative to 120 K, obtaining up to seven monolayers of surface hydrogen upon reaction at 110 K versus less than two monolayers upon reaction at 120 K. Similar differences are also seen at 110 vs 120 K in the amount of Ge deposited on the surface. The increased residence time of digermane at 110 K results in a higher steady-state coverage of physisorbed digermane; this in turn permits more radicals (GeH_3,GeH_2, H, as well as Ge_2H_5 and Ge_2H_4) to be produced upon UV excitation, enabling greater reaction with the dangling bonds present on Si(111). At higher Ge_2H_6 and UV exposures, formation of an amorphous-Ge:H network can result. For the post-UV excitation measurements shown in Figure 1B, we estimate that initially (i.e., low exposures), nearly 100% of the physisorbed digermane reacts upon ultraviolet irradiation. This suggests that competing processes such as photodesorption are not occurring.

It is interesting to speculate as to why post-UV irradiation gave the larger photoenhancement at 110 K while simultaneous UV irradiation gave the larger photoenhancement at 120 K. It is plausible that simultaneous UV exposure should enhance the reactivity of digermane more than post-UV exposure at 120 K, since this temperature is near that of the molecular desorption state (estimated to be between 130 and 145 K). Under post-UV excitation, the coverage of physisorbed digermane begins to decrease at 120 K immediately after the digermane dose has stopped, leaving less digermane to photoreact. The 120 K behavior seen here is similar in nature but lower in extent of reaction than that observed for disilane on Si(100)[59] and Si-(111).[61] The lower reactivity is likely related to the lower molecular desorption temperature (and hence shorter residence time) for digermane versus disilane.

The growth enhancement at 110 K upon photoexcitation of digermane is about 2-fold greater than that observed for disilane on Si(100)[59] and Si(111),[61] suggesting that the photoreactivity of digermane is greater than that of disilane. A strong photoreactivity for post-UV irradiation was also seen for digermane on Si(100)-2×1:D surfaces,[44] compared to that for disilane on the same surface.[59] In the disilane systems, the weak post-UV effect was mainly attributed to the photodesorption of disilane condensed on the surface. Collectively, these observations indicate that the photodesorption channel is probably not as active for digermane as it is for disilane, and/or the photodecomposition channel for digermane is enhanced relative to that for disilane. Li et al.[23] similarly observed an enhanced UV absorption cross-section for digermane relative to disilane. Wright and Hasselbrink[75] have also recently observed dramatic changes upon small temperature variations in the adsorption behavior of disilane adsorbed on D/Si(100) at 99 K versus 108 K. Although the temperature variation in both their study[75] and our study are relatively small, we believe that the data are reflecting changes in molecular reactivity.

At 110 K the percent Ge surface coverages as determined by AES (Figure 3C) for post-UV and simultaneous UV exposure conditions look similar, with both measurements appearing nearly identical at high Ge_2H_6 exposures. In addition, the AES curves level off while the hydrogen desorption yield for the post-UV measurement is increasing (cf. Figure 3A,C) at high Ge_2H_6 exposures. In a related study[65] of the growth behavior of Ge on Si(111), it is suggested that the growth mode of Ge photochemically deposited on Si(111) is best described as Stranski−Krastanov (S−K) growth with Si−Ge intermixing or Volmer−Weber (V−W) growth. Such growth processes would explain why the Ge is not being fully detected by the AES measurements shown in Figure 3C.

4.4. Nature of the Photoassisted Deposition Layer. Two characteristics of the layer deposited using photoexcitation are (i) the production of germane upon heating, and (ii) an enhancement in the hydrogen content of the surface. At the exposure conditions used, germane is not produced without photoexcitation, yet the extent of germane production following UV-assisted growth at 110 K is extensive. We have previously shown that photoexcitation of digermane leads to production of the diradical germylene, GeH_2, which readily inserts into Si−H or Ge−H bonds.[44] The diradical can also insert into Si−Si or Ge−Ge bonds at the surface or in the growing overlayer. It is also well established that silane or germane production upon heating Si or Ge surfaces is due to the presence of silyl (SiH_3) or germyl (GeH_3) species on the surface.[44,53,59,76]

The evolution of extensive GeH_4 and up to 7.3 monolayers of H_2 following a (corrected) dose of 10 langmuirs of digermane suggests that photoexcitation leads to a-Ge:H production. In related systems in which low-temperature, filament-assisted growth was studied, it was found that a-Si:H[77,78] or a-SiC:H[79] could be grown from disilane or methylsilane, respectively. These layers contained a polysilane $(Si-Si)_n$ backbone and contained a mixture of SiH, SiH_2, and SiH_3 within the amorphous network. Similarly, these layers evolved hydrogen and silane when heated, forming a μ-c Si or SiC overlayer. Analogously, we expect that, at the low-temperature photoreaction conditions utilized here, we deposit an a-Ge:H overlayer consisting of a polygermane $(Ge-Ge)_n$ backbone containing GeH, GeH_2, and GeH_3 groups. This overlayer decomposes upon heating to evolve germane and hydrogen, to form Ge−Ge and Si−Ge bonds and, depending upon annealing temperature, to generate a crystalline overlayer.

5. Conclusions

The photoinduced reaction of digermane with Si(111) has been studied at 110 and 120 K. Ultraviolet irradiation during or after digermane exposure enhances the reactivity of digermane on Si(111) compared to similar exposures without UV irradiation. There was greater reactivity of digermane at 110 K than at 120 K for any of the three exposure schemes investigated (simultaneous UV exposure, post-UV exposure, and no-UV exposure). At 110 K, post-UV irradiation enhanced the deposition of germanium more than simultaneous UV irradiation, while the opposite was true at 120 K. Thermally, the reactivity is controlled by the surface dangling bonds; whereas the photoinduced deposition chemistry involves reaction of photogenerated radicals produced in the physisorbed (multi)layer. The low-temperature photodeposition leads to production of an a-Ge:H overlayer that evolves hydrogen and germane upon heating.

Acknowledgment. We gratefully acknowledge support of this research by the Office of Naval Research (N00014-91-J-1432) and the National Science Foundation (DMR-9801024). We thank Stacey F. Bent for a critical reading of the manuscript. We also thank Jeff Kingsley and John C. Hemminger for use of the "desorb" TPD software. This work is dedicated to Professor Kent Wilson. His creativity, enthusiasm, and passion for life, adventure, and scientific discovery are a daily inspiration.

References and Notes

(1) Meyerson, B. S. *Sci. Am.* **1994**, *270*, 62−67.
(2) Mokler, S. M.; Joyce, B. A. *Surf. Sci.* **1993**, *298*, 43−49.

(3) Motta, N.; Sgarlata, A.; De Crescenzi, M.; Derrien, J. *Appl. Surf. Sci.* **1996**, *102*, 57−61.
(4) Minoda, H.; Yagi, K. *J. Cryst. Growth* **1996**, *163*, 48−53.
(5) Xie, M. H.; Zhang, J.; Mokler, S. M.; Fernandez, J.; Joyce, B. A. *Surf. Sci.* **1994**, *320*, 259−270.
(6) Muller, E.; Nissen, H. U.; Ospelt, M.; Von Kanel, H.; Stadelmann, P. *Thin Solid Films* **1989**, *183*, 165−170.
(7) Fukatsu, S.; Fujita, K.; Yaguchi, H.; Shiraki, Y.; Ito, R. *Appl. Phys. Lett.* **1991**, *59*, 2103-2105.
(8) Eberl, K.; Friess, E.; Wegscheider, W.; Menczigar, U.; Abstreiter, G. *Thin Solid Films* **1989**, *183*, 95−103.
(9) Tamagawa, T.; Shintani, T.; Ueba, H.; Tatsuyama, C.; Nakagawa, K.; Miyao, M. *Thin Solid Films* **1994**, *237*, 282−290.
(10) Ohtani, N.; Mokler, S. M.; Xie, M. H.; Zhang, J.; Joyce, B. A. *Surf. Sci.* **1993**, *284*, 305−314.
(11) Ohtani, N.; Mokler, S. M.; Joyce, B. A. *Surf. Sci.* **1993**, *295*, 325−334.
(12) Mokler, S. M.; Ohtani, N.; Xie, M. H.; Zhang, J.; Joyce, B. A. *J. Vac. Sci. Technol. B* **1993**, *11*, 1073−1076.
(13) Yun Li, G.; Hembree, G. G.; Venables, J. A. *Appl. Phys. Lett.* **1995**, *67*, 276−278.
(14) Nakai, K.; Gotoh, Y.; Ozeki, M.; Nakajima, K. *Appl. Surf. Sci.* **1992**, *60/61*, 602−607.
(15) Godbey, D. J.; Lill, J. V.; Deppe, J.; Hobart, K. D. *Appl. Phys. Lett.* **1994**, *65*, 711−713.
(16) Ohtani, N.; Mokler, S. M.; Xie, M. H.; Zhang, J.; Joyce, B. A. *Appl. Phys. Lett.* **1993**, *62*, 2042−2044.
(17) Wado, H.; Shimizu, T.; Ishida, M.; Nakamura, T. *J. Cryst. Growth* **1995**, *147*, 320−325.
(18) Malta, D. P.; Posthill, J. B.; Markunas, R. J.; Humphreys, T. P. *Appl. Phys. Lett.* **1992**, *60*, 844−846.
(19) Ashikaga, K.; Ohno, M.; Nakamura, T.; Fukuda, H.; Ohno, S. *Appl. Surf. Sci.* **1992**, *60/61*, 597−601.
(20) Koschinski, W.; Dettmer, K.; Kessler, F. R. *J. Appl. Phys.* **1992**, *72*, 471−477.
(21) Yasuda, Y.; Koide, Y.; Furukawa, A.; Ohshima, N.; Zaima, S. *J. Appl. Phys.* **1993**, *73*, 2288−2293.
(22) Rowe, J. E.; Riffe, D. M.; Wertheim, G. K.; Bean, J. C. *J. Appl. Phys.* **1994**, *76*, 4915−4917.
(23) Li, C.; John, S.; Banerjee, S. *J. Electron. Mater.* **1995**, *24*, 875−884.
(24) Meyerson, B. S.; Uram, K. J.; LeGoues, F. K. *Appl. Phys. Lett.* **1988**, *53*, 2555.
(25) Ning, B. M. H.; Crowell, J. E. *Appl. Phys. Lett.* **1992**, *60*, 2914−2916.
(26) Ning, B. M. H.; Crowell, J. E. *Surf. Sci.* **1993**, *295*, 79−98.
(27) Hibino, H.; Ogino, T. *Appl. Surf. Sci.* **1994**, *82/83*, 374−379.
(28) Ohshima, N.; Koide, Y.; Zaima, S.; Yasuda, Y. *J. Cryst. Growth* **1991**, *115*, 106−111.
(29) De Crescenzi, M.; Gunnella, R.; Bernardini, R.; De Marco, M.; Davoli, I. *Phys. Rev. B* **1995**, *52*, 1806−1815.
(30) Kajiyama, K.; Tanishiro, Y.; Takayanagi, K. *Surf. Sci.* **1989**, *222*, 38−46.
(31) Wintterlin, J.; Avouris, P. *J. Chem. Phys.* **1994**, *100*, 687−704.
(32) Van, S.; Steinmetz, D.; Bolmont, D.; Koulmann, J. J. *Phys. Rev. B* **1994**, *50*, 4424−4429.
(33) Kajiyama, K.; Tanishiro, Y.; Takayanagi, K. *Surf. Sci.* **1989**, *222*, 47−63.
(34) Shinoda, Y.; Shimizu, N.; Hibino, H.; Nishioka, T.; Heimlich, C.; Kobayashi, Y.; Ishizawa, S.; Sugii, K.; Seki, M. *Appl. Surf. Sci.* **1992**, *60/61*, 112−119.
(35) Carlisle, J. A.; Miller, T.; Chiang, T. C. *Phys. Rev. B* **1994**, *49*, 13600−13606.
(36) Stauffer, L.; Van, S.; Bolmont, D.; Koulmann, J. J.; Minot, C. *Surf. Sci.* **1994**, *307/308*, 274−279.
(37) Mo, Y. W.; Lagally, M. G. *J. Cryst. Growth* **1991**, *111*, 876−881.
(38) Khor, K. E.; Das Sarma, S. *Phys. Rev. B* **1994**, *49*, 13657−13662.
(39) Hammar, M.; LeGoues, F. K.; Tersoff, J.; Reuter, M. C.; Tromp, R. M. *Surf. Sci.* **1996**, *349*, 129−144.
(40) Lapiano-Smith, D. A.; McFeely, F. R. *Thin Solid Films* **1993**, *225*, 187−190.
(41) Coon, P. A.; Wise, M. L.; George, S. M. *Surf. Sci.* **1992**, *278*, 383−396.
(42) Greenlief, C. M.; Wankum, P. C.; Klug, D. A.; Keeling, L. A. *J. Vac. Sci. Technol. A* **1992**, *10*, 2465−2469.
(43) Klug, D. A.; Du, W.; Greenlief, C. M. *J. Vac. Sci. Technol. A* **1993**, *11*, 2067−2072.
(44) Isobe, C.; Cho, H. C.; Crowell, J. E. *Surf. Sci.* **1993**, *295*, 117−132.
(45) Lu, G. Q. In *Group IV Semiconductor Surface Chemistry: A Multiple Internal Reflection Infrared Spectroscopy Study*; Lu, G. Q., Ed.; University of California, San Diego: La Jolla, CA, 1992; p 212.
(46) Uram, K. J.; Jansson, U. *Surf. Sci.* **1991**, *249*, 105−116.
(47) Crowell, J. E.; Lu, G. Q. Epitaxial Heterostructures. *Mater. Res. Soc. Symp. Proc.* **1990**, *198*, 533−538.
(48) Crowell, J. E.; Lu, G. Q. *J. Electron Spectrosc. Relat. Phenom.* **1990**, *54*, 1045−1057.
(49) Lu, G. Q.; Crowell, J. E. Superlattice Structures and Devices. *Proc. Electrochem. Soc.* **1990**, *90−15*, 450−455.
(50) Crowell, J. E.; Lu, G. Q.; Ning, B. M. H. Chemical Perspectives of Microelectronic Materials II. *Mater. Res. Soc. Symp. Proc.* **1991**, *204*, 253−263.
(51) Lu, G. Q.; Crowell, J. E. Manuscript in preparation.
(52) Suda, Y.; Lubben, D.; Motooka, T.; Greene, J. E. *J. Vac. Sci. Technol. A* **1990**, *8*, 61−67.
(53) Imbihl, R.; Demuth, J. E.; Gates, S. M.; Scott, B. A. *Phys. Rev. B* **1989**, *39*, 5222−5233.
(54) Bozso, F.; Avouris, P. *Phys. Rev. B* **1988**, *38*, 3943-.
(55) Avouris, P.; Bozso, F. *J. Phys. Chem.* **1990**, *94*, 2243−2245.
(56) Boland, J. J. *Phys. Rev. B* **1991**, *44*, 1419-.
(57) Kulkarni, S. K.; Gates, S. M.; Scott, B. A.; Sawin, H. H. *Surf. Sci.* **1990**, *239*, 13−25.
(58) Kulkarni, S. K.; Gates, S. M.; Greenlief, C. M.; Sawin, H. H. *Surf. Sci.* **1990**, *239*, 26−35.
(59) Isobe, C.; Cho, H. C.; Crowell, J. E. *Surf. Sci.* **1993**, *295*, 99−116.
(60) Ning, B. M. H.; Crowell, J. E. Manuscript in preparation.
(61) Batinica, G. J.; Crowell, J. E. *J. Phys. Chem. B* **1998**, *102*, 4135−4142.
(62) Crowell, J. E.; Lu, G. Q.; Ning, B. M. H. Atomic Layer Growth and Processing. *Mater. Res. Soc. Symp. Proc.* **1991**, *222*, 189−194.
(63) Boishin, G.; Surnev, L. *Surf. Sci.* **1996**, *345*, 64−74.
(64) Russell, N. M.; Ekerdt, J. G. *Surf. Sci.* **1996**, *369*, 51−68.
(65) Batinica, G. J.; Crowell, J. E. Manuscript in preparation.
(66) Crowell, J. E.; Tedder, L. L.; Cho, H. C.; Cascarano, F. M.; Logan, M. A. *J.Vac. Sci. Technol. A* **1990**, *8*, 1864−1870.
(67) Davis, L. E.; McDonald, N. C.; Palmberg, P. W.; Riach, G. E.; Weber, R. E. *Handbook of Auger Electron Spectroscopy*; Perkin-Elmer Corp., Physical Electronics Division: Eden Prairie, MN, 1978.
(68) Surnev, L.; Tikhov, M. *Surf. Sci.* **1984**, *138*, 40.
(69) McGuire, G. E. *Semiconductor Materials and Process Technology Handbook*; Noyes Publications: Park Ridge, NJ, 1988.
(70) Huang, K. H.; Ku, T. S.; Lin, D. S. *Phys. Rev. B—Condens. Matter* **1997**, *56*, 4878−4886.
(71) Kellerman, B. K.; Mahajan, A.; Russell, N. M.; Ekerdt, J. G.; Banerjee, S. K.; Tasch, A. F.; Campion, A.; White, J. M.; Bonser, D. J. *J. Vac. Sci. Technol. A* **1995**, *13*, 1819−1825.
(72) Gates, S. M. *Surf. Sci.* **1988**, *195*, 307−329.
(73) Lu, G. Q.; Crowell, J. E. *J. Chem. Phys.* **1993**, *98*, 3415−3421.
(74) Lu, G. Q.; Crowell, J. E. Unpublished data.
(75) Wright, S.; Hasselbrink, E. Submitted to *J. Chem. Phys.*
(76) Dillon, A. C.; Robinson, M. B.; George, S. M. *Surf. Sci.* **1993**, *295*, L998−L1004.
(77) Lee, S. S.; Kong, M. J.; Bent, S. F.; Chiang, C. M.; Gates, S. M. *J. Phys. Chem.* **1996**, *100*, 20015−20020.
(78) Chiang, C. M.; Gates, S. M.; Lee, S. S.; Kong, M. J.; Bent, S. F. *J. Phys. Chem. B* **1997**, *101*, 9537−9547.
(79) Lee, S. S.; Bent, S. F. *J. Phys. Chem. B* **1997**, *101*, 9195−9205.